

Depolarized FRET (depolFRET) on the cell surface: FRET control by photoselection

László Bene^{*}, Péter Gogolák[§], Tamás Ungvári[†], Miklós Bagdány[&], István Nagy[#], László Damjanovich^{*}

^{*}Department of Surgery, Faculty of Medicine, University of Debrecen, Debrecen, Hungary

[§]Department of Immunology, Faculty of Medicine, University of Debrecen, Debrecen, Hungary

[†]Department of Biophysics and Cell Biology, Faculty of Medicine, University of Debrecen, Debrecen, Hungary

[&]Department of Physiology, McGill University, Montreal, Canada

[#]Division of Electronics, Research Center for Nuclear Physics of the Hungarian Academy of Sciences, Debrecen, Hungary

Key words: polarizationally structured light, circularly polarized light, diagonal-polarization, Cornu-depolarizer, orientation factor for FRET, homo-FRET

Running title: Twisted FRET

Abbreviations: FRET, fluorescence resonance energy transfer; MHCI/MHCII, Class I/Class II Major Histocompatibility Complex proteins I and II; β_2m , beta-2 microglobulin, the light chain (l.c.) component of MHCI; mAb, monoclonal antibody

Corresponding author: Dr. László Bene, Department of Biophysics and Cell Biology, University of Debrecen, H-4012 Debrecen P.O. Box 39, Hungary, Tel/Fax: (0036)52-412-623, e-mail: bene@med.unideb.hu

Abstract

Sensitivity of FRET in hetero- and homo-FRET systems on the photoselected orientation distribution of donors have been proven by using polarized and depolarized light for excitation. FRET as well as donor and acceptor anisotropies have been simultaneously measured in a dual emission-polarization scheme realized in a conventional flow cytometer by using single laser excitation and applying fluorophore-conjugated mAbs against the MHCI and MHCII cell surface receptors. Depolarization of the originally polarized light have been achieved by using crystal depolarizers based on Cornu's principle, a quarter-wave plate for circular polarization, and a parallel beam splitter acting as a diagonal-polarizer for dual-polarization excitation. Simultaneous analysis of intensity-based FRET efficiency and acceptor depolarization equivocally report that depolarization of light may increase FRET in an amount depending on the acceptor-to-donor concentration ratio. Acceptor depolarization turned to be more sensitive to FRET than donor hyper-polarization and even than intensity-based FRET efficiency. It can be used as a sensitive tool for monitoring changes in the dynamics of the donor-acceptor pairs. The basic observations of FRET enhancement and increased acceptor depolarization obtained for hetero-FRET are paralleled by analogue observations of homo-FRET enhancements under depolarized excitation. In terms of the orientation factor for FRET, the FRET enhancements on depolarization in the condition of the macroscopically isotropic orientation distributions such as those of the cell surface bound fluorophores, report on the presence of local orientation mismatches of the donor and acceptor preventing the optimal FRET in the polarized case, which may be eliminated by the excitation

depolarization. A theory of fluorescence anisotropy for depolarized excitation is also presented.

Introduction

Fluorescence resonance energy transfer (FRET) is a highly sensitive and versatile tool for monitoring orientation and distance changes of fluorophores located at 1-10 nm separations. Due to this attribute, FRET is extensively used for monitoring conformational changes and proximities of biological macromolecules, even in these days in the era of super resolution microscopes. For efficient FRET between a pair of fluorophores, essentially 3 main requirements should be fulfilled: (i) Large overlap between the spectra of donor emission and acceptor absorption on the wavelength scale, (ii) small enough distance between the fluorophores dictated by the above overlap, and (iii) favorable orientation between the fluorophores formulated by the constraint called “orientation factor for FRET” (κ^2) [1-5]. Because the subject of this work is the exploitation of this orientation constraint for a more optimized FRET detection, and because excellent literature is available for FRET theory, we explain only this last parameter in more detail. Without going into quantitative details, the orientation factor expresses the fact that FRET for a given donor-acceptor separation and spectral overlap is favorable only for certain relative orientations of the donor and acceptor dipoles and their joining line, and unfavorable for the others, with the consequence that, for a given donor orientation FRET proceeds only towards those acceptors having the favorable orientations [6-8]. This also means that after the 1st photoselection process of creating the orientation distribution of the excited donors by the exciting light, there exists a 2nd photoselection process of creating the orientation distribution of the excited acceptors by the donor’s local electric field [10-14]. Due to this 2nd photoselection, the orientation distribution of the FRET-excited acceptors may be affected by the orientation distribution of donors, i.e. FRET may happen only towards those acceptors having proper orientations. This property of FRET can also be conceived as an orientation switch for the migrating excitation energy. In the past, this property have been exploited by several researchers for optimizing FRET detection: creating FRET between certain donor and acceptor dyes, one of which can be considered as an isotropic emitter or absorber, e.g. lanthanides with degenerate transitions, phycobiliproteins (Phycocerythrin) with tandem dyes, and quantum dots (QDs) [8, 12, 13].

The orientational optimization of FRET – i.e. making the FRET process independent from the relative donor-acceptor orientations – in these schemes is on the single fluorophore level, by choosing isotropic donors and/or acceptors. However, similar optimization of FRET can also be carried out on the ensemble level of the primarily photoselected donor fluorophores. An indication for that this may be possible can be found in the elegant paper of Corry *et al.* [15], who have clearly shown that membrane bound dyes may have anisotropic local orientation distributions, in spite of the fact that, the whole ensemble of fluorophores can be considered as an isotropically distributed one. They also nicely demonstrate that this local anisotropy manifests itself in anisotropic absorption of light due to photoselection, which can be utilized for determining limits on the orientation factor for FRET, the κ^2 . Taking into account that FRET depends on the relative donor-acceptor orientations (“2nd photoselection”) similarly to the way absorption depends on the relative photon field-dye orientations, the implication of these observations is that, not only the absorption process, but also the FRET process may be sensitive to the anisotropy of orientation distributions in polarized exciting light. As a closer inspection, taking now two anisotropically distributed types of dyes – the donors and the acceptors – bound to membrane receptors, it is expected that for polarized excitation only for donor acceptor dyes pairs found in specific locations of the cell membrane will FRET be optimal (Fig. 1) [15, 16]. In contrast, for depolarized excitation each position in

the cell membrane can be taken as equivalent concerning FRET, an indication for an enhanced sensitivity of FRET detection in depolarized exciting light.

For achieving a more complete description of the FRET effects of depolarized excitation a dual-polarization detection scheme (“Single laser polFRET”) has been applied in a flow cytometer, where in addition to the FRET efficiency, donor and acceptor anisotropies are also detected on a cell-by-cell basis [17]. Hyper-polarization of donor anisotropy is expected whenever FRET efficiency increases, due to the lifetime shortening of the donors. On the acceptor side, however, a reduction of anisotropy is expected due to the depolarized excitation by FRET. Although both anisotropies change with FRET, acceptor anisotropy is expected to be more sensitive than the donor anisotropy. While the donor anisotropy reflects FRET mainly through the lifetime reduction, acceptor anisotropy may also change when only the anisotropy of sensitized emission changes and the FRET efficiency itself stays constant. Another use of this detection scheme, that it enables the computation of the orientation factor (κ^2) for FRET [18, 19].

Depolarization – understood in the plane transversal to the direction of light propagation – of the inherently polarized laser light has been accomplished by using different phase retarder crystals and by a parallel beam-splitter (“Savart plate”). (i) The Cornu#1-depolarizer – two birefringent prisms cemented together through their wedge faces – introduces a gradual change in polarization through the beam diameter. Although, the polarization state of the exciting light is spatially modulated in this case (“pseudo-depolarization”) at a rate dictated by the wedge angle, the averaged vanishing polarization is observed due to the motion of the cells through the laser beam [20-22]. (ii) The depolarizer Cornu#2 (also designated as “wedge”), is also based on the above Cornu’s principle with the same wedge angle as for Cornu#1, but that is a smaller crystal having larger intensity loss. (iii) A quarter-wave plate ($\lambda/4$ -plate), turning linear polarization into circular polarization. (iv) A parallel beam-splitter (diagonal-polarizer, cross-polarizer or Savart-plate) [23], turning the incoming linearly polarized light into two perpendicularly polarized ones proceeding in parallel with intensities dictated by the angle between the polarization direction of the incoming beam and the fast axis of the front face of the crystal. Here the deviation of the two beams is small enough to be shown up as a single beam in these experiments. Although these crystals might enable completely depolarized excitation in the plane perpendicular to the illumination direction, the detected fluorescence might remain only partially depolarized due to the perpendicular observation direction of the flow cytometer [24, 25]. This feature enables the reconstruction of the same anisotropies obtainable by the “conventional” linearly polarized excitation with a slight modification of the algorithm for anisotropy determination – please see it in *Supporting information*.

Our biological test system is comprised of the MHCI and MHCII cell surface receptors labeled with fluorescently conjugated mAbs on the JY B lymphoblast cells [26-29]. These receptors are key players of adaptive immunity in orchestrating immune recognition processes between cells. In addition to the high surface expression levels – ensuring good signal-to-noise ratios important in the polarized FRET measurements – these receptors form high degree of homo- and hetero-associations, proven by us earlier using different FRET and microscopic colocalisation approaches. An advantage of this system, that the acceptor-to-donor dye ratio at the cell surface, a key factor determining FRET, can be adjusted by the dye-per-protein ratios of the mAbs – besides the expression levels of these receptors – at custom making possible investigation of the FRET effects as the function of the acceptor-to-donor ratio. Further versatility for modulating the acceptor-to-donor ratio is offered by simultaneously labeling with multiple donor and acceptor mAbs, which has been used also in this study. This system can also be utilized for testing the behavior of homo-FRET under depolarized excitation [30].

Materials and methods

Cell line, monoclonal mAbs, fluorescent staining of mAbs, labeling of cells with mAbs, and determination of expression levels of receptors (in Supporting information).

Flow cytometric dual-anisotropy measurements

Cell-by-cell basis correlated measurements of the polarized intensity components of the donor and acceptor were carried out in a „dual T-format” arrangement [24, 31, 32]. It was realized in a modified FACStar^{Plus} flow cytometer (Becton Dickinson, CA) by placing two polarization beam splitter cubes (broadband polarization beam-splitter cube, model 10FC16PB.3, Newport) in the donor and acceptor fluorescence channels (Fig. 2). The fluorescence intensities of the green (Alexa-Fluor 488, A488) donor dye and the red acceptor dye (Alexa-Fluor 546, A546) were excited with an Argon-ion laser (Model Stabilite-2017, Spectra Physics, Mountain View, California) in all-lines mode – comprised mainly of 488 nm- and 514 nm-light – and were detected orthogonally to the direction of the exciting laser light beam by green and red sensitive photomultiplier tubes (Hamamatsu). The all-lines mode was used for improving signal-to-noise ratio for the anisotropy detection as well as to improve the quality of depolarization by reducing coherence with the diagonal polarizer. After transmitting through a 525-nm long path filter to reduce background due to the light scattering (HQ525 lp, all HQ filters used were manufactured by AF Analysentechnik, Tübingen) the donor and acceptor fluorescence intensities were partially separated by a suitable dichroic mirror (DM in Fig. 2, manufactured by Ferenc Kárpát, Central Physics Research Institute, Budapest, Hungary), and subsequently detected either at 535 ± 15 nm (fluorescence channel of the donor, channel#1) or at 640 ± 60 nm (fluorescence channel of the acceptor, channel#2) (filters HQ535/30 bp and HQ 640/120 bp). The donor and acceptor fluorescence intensities were further split by two identical broadband polarization beam splitter cubes (10FC16PB.3, Newport) into their vertical and horizontal components before reaching the respective photomultipliers.

Depolarizers and polarization modes of excitation

First the “vertical” and “horizontal” linearly polarized excitation modes have been fixed relative to the polarization directions of the detection channels with the aid of a Fresnel-type double-rhomb polarization rotator (broadband polarization rotator, model PR-550, Newport) using direct laser light reflection, 90° light scattering, or fluorescence [33]. The “vertical” direction of excitation was defined by the condition that the signal in the horizontal channel should be minimal with this mode of excitation. Then, for the determination of the G_i -factors ($i=1, 2$) for the fluorescence channels, the vertical polarization direction of laser light was rotated by 90° with the polarization rotator. These G_i factors were used for calculating the anisotropies with all excitation modes. The following crystals have been used for depolarization of the exciting light: Cornu#1, Cornu#2 depolarizers both from Melles Griot (Farnham, Surrey, England), and achromatic quarter-wave plate (#1140, 10 mm aperture, 400-750 nm), quartz parallel polarizing splitter (“cross or diagonal polarizer”, #9472, 10x10 mm, 50 μ m displacement at 633 nm) the latter two from United Chrystals. The depolarizing crystals have been mounted on the rotator outlet, and first their fast axis direction has been found by minimization of the signal in the horizontal channel at the vertically oriented output of the rotator. Subsequently, the depolarized excitation modes have been defined by orienting the fast axis directions at 45° to the “vertically” oriented output of the rotator.

Methods for excitation depolarization (in Supporting Information)

Signal processing

For each excitation mode – linearly polarized and depolarized – two polarized intensities have been detected for each fluorescence channel: I_{iv} , I_{ih} , with the first index i designating the signal channel ($i=1$, donor; 2 acceptor), the second one referring to the polarization direction of the detected fluorescence, respectively. These same signals have been recorded for each excitation mode and kind of sample (background, donor only, acceptor only, and doubly labeled). The way of data processing however depended on the mode of excitation.

Horizontally polarized excitation (Fig. 3, Panel A): After subtracting the corresponding background intensities measured on the unlabeled cells from the polarized intensities, the correction factors G_i ($i=1, 2$) balancing the sensitivities of vertical and horizontal fluorescence channels were calculated as follows:

$$G_i = I_{iv}/I_{ih} . \quad (1)$$

Vertically polarized excitation (Fig. 3, Panel B): Then the total fluorescence intensities I_i , and the fluorescence anisotropies r_i were calculated as follows:

$$I_i = I_{iv} + a(\psi) \cdot G_i \cdot I_{ih} , \quad (2)$$

$$r_i = (I_{iv} - G_i \cdot I_{ih})/I_i . \quad (3)$$

In the above expression for the total intensities I_i ($i=1,2$) a numerical correction for the high aperture fluorescence collection was carried out according to T.M. Jovin [30, 34] by using the term $a(\psi) = 1 + \cos\psi \cdot (1 + \cos\psi)/2$, where $a(\psi)$ assumes a value of 1.72 for our numerical aperture of NA=0.6, and ψ stands for the half angle of the detected light cone. Based on Eq. 2 the r_{corr} aperture-corrected anisotropy can be written as the function of the r uncorrected one as follows: $r_{corr} = 3 \cdot r / \{1 + a(\psi) + r \cdot [2 - a(\psi)]\}$.

Depolarized excitation (Fig. 3, Panel D): For this excitation mode, signals detected in the direction of illumination are depolarized, but those detected at sideways are partially polarized [24, 25]. This makes possible the computation of total intensities and anisotropies like in the vertical excitation case, but in modified forms:

$$I_i = 2 \cdot I_{iv} + [a(\psi) - 1] \cdot G_i \cdot I_{ih} , \quad (4)$$

$$r_i = 2 \cdot (I_{iv} - G_i \cdot I_{ih})/I_i . \quad (5)$$

Formally the total intensity and anisotropy can also be computed according to Eqs. 2, 3, but this way the real quantities (Eqs. 4, 5) are underestimated. If the quantities computed according Eqs. 2, 3 are designated by I_i' , and r_i' then these can be traced to the above I_i , and r_i as follows:

$$I_i' = (2 - r_i) \cdot I_i / 2 , \quad (6)$$

$$r_i' = r_i / (2 - r_i) . \quad (7)$$

By inspecting Eqs. 6, 7 it can be seen that by calculating the conventional manner (Eqs. 2, 3) both total intensity and anisotropy are underestimated in an anisotropy (r_i) dependent fashion. For the deduction of these relations please see the end of *Supporting information*.

Diagonally polarized excitation (Fig. 3, Panel C): Interestingly, the way of calculation of anisotropy and total intensity is the same as for the depolarized light, so Eqs. 4, 5 are also valid for this case, based on the fact that depolarized light can be obtained from the cross-polarized (or diagonally polarized) one – and also from the linearly polarized one – by random rotations. Please see the proof at the end of *Supporting information*.

The anisotropy and total intensity values for each excitation mode were computed on a cell-by-cell basis from the correlated I_{iv} and I_{ih} intensities with predetermined values of the G_i factors ($i=1, 2$) as input parameters. The mean values of fluorescence anisotropy and total intensity histograms measured on the single donor- or acceptor-labeled cells ($\sim 10^4$) were further used for the calculation of the necessary input constants α , S , S_1 , $f_{a/d}$, r_a for constructing the histograms of different quantities determined from the double-labeled FRET samples such as the set of quantities E , r_a' , r_{et} , and T (Eqs. 8-11). The average values of the means of anisotropy histograms obtained in different measurements with their standard errors were also determined and are listed in Table 1 of the main text, and Tables 1s, 2s in the *Supporting information*. The generation and subsequent analysis of flow cytometric histograms and 2-dimensional correlation plots (dot-plots) of total fluorescence intensities, fluorescence anisotropy, and FRET efficiency (Figs. 4-7) were performed by a home-made software specialized for flow cytometric data analyses called Reflex, written by G. Szentesi [35], freely downloadable from <http://www.biophys.dote.hu/research.htm>, and <http://www.freewebs.com/cytoflex.htm>, or from the corresponding author bene@med.unideb.hu.

Theoretical results

Quantities of the single laser polFRET method

The FRET consequences of the depolarized excitation has been investigated in the framework of the “Single laser polFRET” method introduced by us earlier [17]. We only list the quantities used in the present work, and please refer to the earlier publication and to the *Supporting information* of this paper for the definitions and the computational details. (i) FRET efficiency E computed from the intensity ratio S_1' ($=I_2/I_1$) in the knowledge of spectral constants α , S_1 , and S , and the acceptor-to-donor ratio parameter $f_{a/d}=I_a/I_d$ predetermined on the single-labeled samples:

$$E = [(S_1' - S_1)/(1 - S \cdot S_1') - f_{a/d}] / [(S_1' - S_1)/(1 - S \cdot S_1') + \alpha]. \quad (8)$$

ii) Donor anisotropies r_d and r' measured in the absence and presence of acceptor. r' is calculated from the directly measured r_1 anisotropy of the 1st channel, the intensity ratio S_1' , and anisotropy r_2 of the 2nd channel by using the spectral constants S , S_1 , ρ_d and ρ_a :

$$r' = (r_1 - S \cdot S_1' \cdot \rho_a \cdot r_2) / (1 - S \cdot S_1') \cdot (1 - S \cdot S_1) / (1 - S \cdot S_1 \cdot \rho_d \cdot \rho_a). \quad (9)$$

Donor anisotropy enhancement ($r' > r_d$) is expected in the presence of FRET. The difference between r' and r_d is an indicator of FRET. (iii) Acceptor anisotropies r_a and r_a' measured in the absence and presence of donor. r_a' is calculated from the directly measured r_1 anisotropy of the 1st channel, the intensity ratio S_1' , and anisotropy r_2 of the 2nd channel by using the spectral constants S , S_1 , ρ_d and ρ_a :

$$r_a' = (S_1' \cdot r_2 - S_1 \cdot \rho_d \cdot r_1) / (S_1' - S_1) \cdot (1 - S \cdot S_1) / (1 - S \cdot S_1 \cdot \rho_d \cdot \rho_a). \quad (10)$$

A decrease in acceptor anisotropy ($r_a' < r_a$) is expected in the presence of FRET. The difference between r_a and r_a' is an indicator of FRET. (iv) Anisotropy of sensitized emission r_{et} is determined from the acceptor anisotropies r_a , r_a' and FRET efficiency E in the knowledge of the spectral sensitivity constant α and the acceptor-to-donor ratio parameter $f_{a/d}$ predetermined on the single-labeled samples:

$$r_{et} = r_a' - f_{a/d} \cdot (r_a - r_a') / (E \cdot \alpha). \quad (11)$$

(v) According to Eq. 11 and point (iii) above the anisotropy ratio r_a'/r_a can be used as a FRET descriptor, however in addition to E it may also depend on the anisotropy of sensitized emission r_{et} , i.e. the relative orientation of the donor and acceptor:

$$r_a'/r_a = (f_{a/d} + E \cdot \alpha \cdot r_{et}/r_a) / (f_{a/d} + E \cdot \alpha). \quad (12)$$

Eq. 12 tells us that the r_a'/r_a ratio changes whenever E or r_{et} , i.e. the relative orientation of the donor and acceptor changes. Based on this property it is a candidate also for measuring conformational changes. Furthermore, if the $r_{et} \ll r_a$ condition is met, the r_a'/r_a ratio might drop with increasing E , because the E -containing 2nd term in the numerator could be vanishingly small. (vi) Another useful FRET indicator is formed by ratioing the anisotropy of the 2nd channel, r_2 , in the presence of FRET and the intensity weighted average, $r_{2,av}$, of the anisotropy of the acceptor labeled sample r_a and that for the donor labeled sample, r_{2d} , also measured in the 2nd channel, i.e.

$$r_{2,av} \equiv (I_{2d} \cdot r_{2d} + I_{2a} \cdot r_a) / (I_{2d} + I_{2a}). \quad (13)$$

This quantity can also be traced to the above defined FRET efficiency E , donor anisotropies r_d , r' , and the acceptor anisotropies r_a and r_{et} by using the predefined spectral constants α , S_1 , r_d and the $f_{a/d}$ parameter as follows:

$$r_2/r_{2,av} = [1 - E \cdot (S_1 \cdot \rho_d \cdot r' - \alpha \cdot r_{et}) / (S_1 \cdot \rho_d \cdot r_d + f_{a/d} \cdot r_a)] / [1 + E \cdot (\alpha - S_1) / (S_1 + f_{a/d})]. \quad (14)$$

This quantity can also be a sensitive indicator of conformational changes because of the involvement of anisotropies in addition to the FRET efficiency. Furthermore the $r_2/r_{2,av}$ ratio is more sensitive to changes in FRET efficiency than the r_a'/r_a ratio, because while in the r_a'/r_a ratio the denominator and numerator change in parallel as functions of E , in the $r_2/r_{2,av}$ ratio they change oppositely. By inspecting Eqs. 12, 14 it can also be seen that E can be determined with anisotropies (it maybe called “polarized FRET efficiency” and designated with T to be distinguished from E) if some assumption on the value or r_{et} is met, e.g. that it is zero. The conventional FRET efficiency E and the “polFRET efficiency” T as expressed in terms of the acceptor anisotropies are the following:

$$E = f_{a/d} / \alpha \cdot (r_a/r_a' - 1) / (1 - r_{et}/r_a'), \quad (15)$$

$$T \equiv f_{a/d} / \alpha \cdot (r_a/r_a' - 1). \quad (16)$$

From these formulae a direct relation between T and E can be deduced,

$$T = E \cdot (1 - r_{et}/r_a'), \quad (17)$$

from which it can be seen that T coincides with E whenever r_{et} equals zero, under-estimates E for positive r_{et} , and upper-estimates it for negative r_{et} .

Homo-FRET enhancement (in Supporting information)

Experimental results

The test system: FRET between MHC Class I and MHC class II molecules

As to the testing FRET systems, we used fluorescently conjugated mAbs L368 and W6/32 binding to the light and heavy chain components of the same MHCI molecule, respectively, as well as an mAb (L243) binding to the MHCII molecule [26]. Substantial FRET efficiencies could be expected for these systems, based on the large degree of proximities of the binding epitopes proven with different methods earlier [26-28]. These two receptors are vital in immune recognition processes. They form extended homo- and hetero-associations favoring signal amplification. For checking on a possible acceptor-to-donor ratio dependence of the expected depolarization effects, we adjusted the acceptor-to-donor ratio by properly choosing the dye-per-protein labeling ratio (D/P or L) of the mAbs taking into account also the receptor expression levels. Besides serving as an alternative way for adjusting the acceptor-to-donor ratio, investigations on the possible effects of photoselection exerted on FRET taking place between identical dyes (homo-FRET) are also aimed by simultaneously labeling with 2 donor or acceptor mAbs. Here information on homo-FRET can be obtained by the excess depolarization of fluorescence of the double-labeled sample compared to those of the single-labeled ones (see also Eq. 13s in Supporting information).

Depolarized excitation enhances efficiency of hetero-FRET and reduces anisotropy of sensitized emission

Data obtained in the single laser polFRET platform for vertically polarized and depolarized excitations are summarized in Table 1, Figs. 4-7 of main text, and Tables 1s, 2s in *Supporting information*. Table 1, Parts A, B cover data obtained with vertically polarized excitation for FRET taking place in the MHCI→MHCII direction (Part A) and in the reversed MHCII→MHCI direction. Two important variables into which all information needed is condensed are the conventional FRET efficiency E (Eq. 8) and the polFRET efficiency T (Eq. 16). The anisotropies are important for the accurate computation of the T variable itself and they can be visualized as the building blocks of T (Eqs. 10, 16).

(i) Polarized excitation: By inspecting Parts A, B it can be seen that significant FRET efficiencies E (all is higher than ~10%) have been measured which are consistent with the high proximity of the MHCI and MHCII cell surface receptors proven earlier by other means [26-29] (see also Fig. 4, Panel A). For revealing possible trends behind the data, the acceptor-to-donor concentration ratios (c_a/c_d) – computed from total donor and acceptor intensities I_{2a} , I_{1d} in the knowledge of the α sensitivity factor as $I_{2a}/(\alpha \cdot I_{1d})$ – have also been listed. It can be seen that both the E and T values follow in parallel the changes in the acceptor-to-donor ratio, as expected for FRET (e.g. ~25% FRET for $c_a/c_d=0.5$ and ~40% for $c_a/c_d=3.5$ in Part A). An interesting feature is that all T values are c.a. the half of the corresponding E values (Fig. 4 Panels A, F; Fig. 5 Panels A, B). Based on the defining formulae for E and T (Eqs. 15-17) this observation can be explained by the nonzero anisotropies of the sensitized emission (r_{et}). The r_{et} values directly computed by using Eq. 11 are consistent with this observation: Albeit smaller than 10%, but definitely nonzero r_{et} values have been measured in the majority of cases (Parts A, B).

As to the other anisotropies (see also Fig. 4), the high anisotropy values (~20% for donors, and somewhat higher ~26% for acceptors) obtained for the singly donor- and acceptor-labeled samples report on that the orientation distribution of the excited donor and excited acceptor is not isotropic on the timescale of fluorescence, implying that their rotational motion is considerably hindered.

The $r_{2,av}$ average anisotropies are calculated as the intensity weighted means of the donor and acceptor anisotropies measured in the acceptor channel (Eq. 13). These are close to the acceptor anisotropies r_a , because the donor contribution in the acceptor channel is generally small. The importance of this variable lies in that together with the r_2 anisotropy measured on the FRET sample, it is used for calculating the anisotropy ratio $r_2/r_{2,av}$ which is a very sensitive quantity for probing changes in FRET due to its direct dependence on both E and r_{et} (Eq. 14).

The importance of acceptor anisotropy r_a lies in that, similarly to the $r_2/r_{2,av}$ ratio, the ratio of r_a'/r_a can also be formed, where r_a' is the acceptor anisotropy measured on the FRET sample in the presence of the FRET and can be used for sensing FRET changes (Eq. 12), but its sensitivity a little smaller than for the $r_2/r_{2,av}$ ratio. Besides sensitively indicating changes in FRET, another significance of these ratios is that although through different formulas, the same “polFRET efficiency” T values can be deduced from both of them (Eqs. 12, 14). This could be read off from the data: Both of the r_2 and r_a' anisotropies measured on the FRET samples are significantly smaller than the corresponding $r_{2,av}$ and r_a values measured in the absence of FRET, i.e. on the single donor- and acceptor-labeled samples. Interestingly, their relative differences ($\delta r_2 \equiv 1 - r_2/r_{2,av}$, and $\delta r_a \equiv 1 - r_a'/r_a$) inversely correlate with E and T , as well as with the acceptor-to-donor ratio (Eqs. 12, 14) (Fig. 4, Panels B-E; Fig. 5, Panels A, C).

When the donor anisotropies r_1' (Eq. 9) measured in the presence of FRET on the doubly-labeled samples are considered (not shown), we obtained values slightly larger than

the corresponding r_d anisotropies of the singly donor-labeled samples, following the trend of E regarding the dependence on the acceptor-to-donor ratio. The donor anisotropy enhancement can be attributed to the shortage of lifetime in the presence of FRET. However, because the acceptor anisotropy is a much more sensitive and accurate FRET indicator than donor anisotropy for these moderate transfer efficiencies we did not tabulate them. The involvement of donor anisotropy in the analysis is justified by the fact that due to the donor overspill into the acceptor channel, it is needed for the accurate computation of the anisotropies r_a' , r_{et} and of the T (Eqs. 10, 16).

(ii) Depolarized excitation: Data on depolarized excitation realized with the Cornu#1 depolarizer are listed in Table 1, Parts C, D. For pertinent flow cytometric histograms, please see Figs. 4-7. By comparing E and T values of the depolarized and vertically polarized cases, it can be seen that although both E and T are significantly enhanced by excitation depolarization the enhancements for T are much larger than for E (~16% for E vs. ~100% for T) (Fig. 4, Panels A, F; Fig. 5 Panels B, D). Additionally the systematic deviation of T from E experienced with vertical excitation disappeared upon depolarized excitation (Fig. 4, Panels A, F; Fig. 5 Panels B, D). Inspecting now the corresponding r_{et} variable, the anisotropy of sensitized emission, we see that its vanishingly small values in the depolarized case partly explains the reducing difference between T and E (Fig. 4, Panels A, E, F). Examining the T and E values as functions of the acceptor-to-donor ratio, it can be seen that the enhancements change inversely with the acceptor-to-donor ratio, with the smallest enhancement belonging to the largest acceptor-donor ratio (~0% for $c_a/c_d=0.35$) and vice versa (~23% for $c_a/c_d=0.07$). This finding is reasonable, because the effect of excitation depolarization is mediated by the donors. As a summary, these observations indicate that, the FRET enhancement effect through photoselection seems to operate in a degree determined by the anisotropy of orientation distributions, and the latter seems to be influenced by the acceptor-to-donor ratio.

As to the anisotropies, we see that although the anisotropies measured with the Cornu#1 depolarizer are systematically smaller than those for the vertical case, they kept the trends in their relative magnitudes observed with the vertical excitation (Fig. 4, Panels B-E; Fig. 5, Panels A, C). The systematic anisotropy deviations can be attributed to possible optical path difference between the two modes of illumination. In our treatment we regard anisotropy values as solely molecular attributes characterized by the fluorescence lifetime, the rotational correlation time, and the limiting anisotropy of the molecule obtainable with linearly polarized excitation according to the Perrin-equation [17]. Consequently, the same values of anisotropies should be recovered, independently of the polarization state of the excitation, albeit through different mathematical formalisms. (With this approach, the conventional form of Perrin equation and the depolarization factors in it have been kept also for depolarized excitation. As an alternative approach the directly measurable anisotropies as calculated by the conventional formulas Eqs. 2, 3 could also be used in the depolarized case, but then the form of Perrin equation, i.e. the form of the depolarization factors would be different.)

The relative change in the “mixed anisotropy” r_2 ($\delta r_2=1-r_2/r_{2,av}$) sensitively decreased (with ~60%) upon depolarized excitation. Similar decreases have been obtained for the relative changes of the r_a acceptor anisotropy ($\delta r_a=1-r_a'/r_a$), however with little larger errors (not shown). That the relative changes of the r_2 and r_a anisotropies are much more sensitive to the excitation depolarization than the corresponding FRET efficiencies E , is supposedly due to the fact that the $r_2/r_{2,av}$ and r_a'/r_a ratios depend on the donor and acceptor anisotropies in addition to the FRET efficiency (Eqs. 12, 14).

Depolarized excitation enhances homo-FRET

A variable similar to the average “mixed anisotropy” of the acceptor channel ($r_{2,av}$) introduced above, the intensity weighted average of the anisotropies of single acceptor-labeled samples,

$r_{a,av}$ has also been introduced. It is important for the computation of the homo-FRET enhancement for the acceptor η (Eqs. 12s, 13s *in Supporting information*). By comparing this average and the acceptor anisotropy measured for the A488-L243→(A546-L368+A546-W6/32) FRET pair, it can be seen that significant homo-FRET ($\eta=17.5\%$) exists between the A546-L368 and A546-W/632 mAbs (Table 1, Part A; Figs. 6, 7). This is reasonable, because the L368 and W6/32 mAbs bind to two different epitopes – the β_2 -microglobulin or light chain (l.c.), and heavy chain (h.c.) components in close (~ 7.5 nm) proximity – of the same MHC I molecule [29].

As to the effect of excitation depolarization on homo-FRET, an enhancement value c.a. the double of that for the vertical case has been observed under depolarized illumination (35% vs. 18%) (Table 1, Parts B, D; Figs. 6, 7). This observation suggests that the enhancement effect might be of a general nature. It can be attributed to opening of new FRET pathways ensured by the more favorable relative orientations of the donor and acceptor under depolarized illumination. However, because the effect is achieved by modulation of the orientation distribution of the excited donors it may depend on the acceptor-donor ratio, besides the degree of anisotropy of the acceptor orientation distribution.

Data for other ways of excitation depolarization: diagonal polarizer, circular polarizer, and Cornu#2 (in Supporting information)

Discussion

Dependence of FRET on dye orientation and anisotropic orientation distributions of dyes in the cell membrane

FRET is inherently directional by the constraint dictated by the orientation factor (κ^2) [6-8, 12, 13, 15, 18, 19, 36]. FRET directionality means that FRET can take place only towards those acceptors having special favorable dipole orientations (Fig. 1). At a given donor-acceptor separation, FRET is maximal for those acceptors having dipole directions parallel with the donor field direction at the position of the acceptor, and zero for those acceptors having dipole directions perpendicular to the donor field. In the language using the dipole direction of the donor instead of the direction of its field vector, this law can also be formulated in an alternative way: FRET is maximal ($\kappa^2=4$) for those donors and acceptors whose dipole directions are parallel with the line connecting the donor and acceptor, and zero for those who are perpendicular to each other and to the connecting line. For freely rotating donors or acceptors – whose rotational correlation time is much smaller than the fluorescence lifetime – or donors having orientationally “mixed transitions” this constraint is meaningless and FRET is isotropic [6-8, 12, 13, 18, 19]. Although this requirement may be fulfilled in some special cases, in the majority of cases directionality of FRET and the value of orientation factor is a subject of consideration [6-8]. Directionality of FRET also means that in addition to the first photoselection of the donor dipoles by the exciting light, there is a second photoselection process by FRET, the photoselection of the excited acceptors by the local field direction of the donor [6-8, 14, 19]. Earlier, for membrane bound dyes targeted via mAbs to cell surface receptors, for the polarized excitations meant by the laser light we and others observed large anisotropies. This indicates that the orientation distributions of the dyes are not isotropic locally in spite of the global isotropy dictated by the symmetry of the whole cell surface. Based on the principle of local anisotropy in the cell membrane, even an anisotropy-free method of deducing orientation distributions of membrane-bound dyes has been worked out in an elegant work by Corry *et al.* [15].

With polarized excitations, orientation distributions of the excited donors – not considering now the afore-mentioned structurally isotropic ones – is always anisotropic irrespective of the nature of orientation distribution of the whole population. Taking now into

account also the directionality of FRET, a degree of local orientation anisotropy of acceptor relative to the membrane surface can lead to local inhomogeneities or spatial variations (“gradients”) in FRET in the cell membrane (Fig. 1) [15, 16]. This spatial inhomogeneity of FRET can be eliminated by using e.g. isotropically oriented acceptors. Alternatively, it can also be influenced by the photoselection of the orientation distribution of the excited donor subpopulation by using differently polarized light beams [9-11].

Single laser polFRET platform

Fitted to the nature of the problem, we collected and analyzed our data in the framework of the “Single laser polFRET” method introduced earlier by us. In addition to the forward angle light scattering signal (FSC) used for separating cells from debris, 4 fluorescence signals, the polarized intensity components of fluorescence of the donor (I_{1vh} , I_{1vv}) and of the acceptor (I_{2vh} , I_{2vv}) have been detected (Fig. 2). From these signals FRET efficiency and the donor and acceptor anisotropies have been calculated in the knowledge of the spectral spillage factors (S , S_1 , ρ_d , ρ_a) the sensitivity constant (α), and the donor-acceptor ratio parameter ($f_{a/d}$) determined from data measured on samples labeled with only donor or acceptor. For the details please see [16], and the *Supporting information* of this article. The suitability of this method for the present purpose lies in that, in addition to supplying information on the degree of randomness of the orientation distributions in the form of anisotropies (r_1 , r_2), it enables also probing the nature of the relative donor-acceptor orientations, via the anisotropy of sensitized emission of the acceptor (r_{et}). Furthermore, a FRET efficiency like parameter called “polFRET efficiency” (T) has also been introduced as a joint measure of FRET efficiency (E) and anisotropy of sensitized emission (r_{et}) (Eq. 17). T coincides with the real FRET efficiency E for zero values of r_{et} and under-estimates E for positive r_{et} values. T is also a candidate for a sensitive sensor of conformational dynamics, because of its capability for simultaneously monitoring proximity (via E) and relative rotations (via r_{et}).

Relevance of depolFRET for probing receptor dynamics

We used the polFRET method merely for a more complete description of the possible effects of photoselection to the detected FRET. However, comparative FRET measurements using polarized and depolarized excitations can also be carried out in simpler detection schemes of FRET, where only the total donor and/or acceptor intensities are considered, e.g. in the dual- or single-laser flow cytometric FRET methods called FCET [37, 38]. However, to avoid possible influence of polarization on the detected signals at the 90° observation direction, the detection optics should be extended with polarizer with its transmission direction oriented at magic angle ($\Theta=54.74^\circ$) to the vertical [17, 24, 34]. FRET between oriented or partially oriented donors and acceptors may change if the donors or acceptors reorient during a conformational change or repatterning of receptor clusters. E.g. the relative difference of FRET efficiencies obtained under polarized and depolarized excitation before and after the conformational change may indicate the direction of the changes in the orientation distributions, i.e. whether they became more anisotropic, or randomized. The principle of depolFRET can also be extended to the time domain. E.g. monitoring FRET under laser excitations alternating between polarized and depolarized modes („ALEX”) could supply information on time variation of orientation distribution of the donor and acceptor [39]. A “polarization rotating microscope” [40, 41] can also be used for this purpose.

Separating contributions of segmental flexibility of bound dyes and orientational distributions of holding receptors to the emission anisotropy and orientation factor

The depolFRET approach also offers the feasibility for the determination of finer details of the orientation distributions of receptor-tethered dyes. Namely separating the contributions of

the tethered motion and the rotation of the holding matrix to the measured fluorescence anisotropy of the dye in the steady state. This kind of rotational heterogeneity traditionally has been resolved by measuring fluorescence anisotropy decays in the time domain or by applying multiple modulation frequencies of the exciting light in differential polarized phase fluorometry.

A starting point for a kind of quantitative analysis can be the orientation factor model of Corry *et al.* [17] who specialized the quantitative form of orientation factor originally given by Dale *et al.* [18] to the characteristics of the orientation distribution of the membrane receptors and the tethering motion of the bound dyes, symbolized respectively by the α_d , α_a and ψ_d , ψ_a polar angles in their formulae, in the Eqs. 29-36 in [17]. Although in their original approach of measuring only the modulation of emission intensity by the detection angle encoded in their B_d and B_a parameters this is not feasible – these quantities being the products of the depolarization factors for the dye tethered motion and the receptor orientation distribution, Eq. 32 in [17] –, it may be attempted by writing up the orientation factor for two differently photoselected – a linearly polarized and a depolarized – donor populations. Although the functional form of the orientation factor should reflect the photoselected donor population, ultimately it should depend on the same input constants (α_d , α_a , ψ_d , ψ_a) characterizing the orientation distributions of the donor and acceptor. As a very crude first approximation, the expression of κ^2 elaborated for donors possessing degenerate transitions in a plane could be used for the depolarized case [6, 12, 13].

By eliminating the ψ_d , ψ_a quantities via expressing them with the primarily measured B_d and B_a quantities, we are left behind with two expressions of the orientation factor for the two unknowns (α_d , α_a). Unfortunately, the values of κ^2 for the different photoselections are also unknown in general. However, in special cases when the donor-acceptor separation is also known, these can be estimated from the measured FRET efficiencies, and the system of equations can be solved for the 2 unknown angles. In the framework of the polFRET method, the intensity modulation parameters B_d and B_a which have an anisotropy character, can be replaced by the fluorescence anisotropies of the donor and acceptor (r_d , r_a). Another degree of freedom offered by the polFRET method is the relative angle of the donor and acceptor orientation distributions, reflected in the anisotropy of sensitized emission (r_{et}). Apart from the known donor-acceptor separations, the validity of this approach depends also on the structural model of the orientation distributions in the framework of which the orientation factor is computed. Crucial points are the assumption on the axial symmetry of the orientation distributions around the membrane normal, and that the donor-acceptor position vector is parallel with the membrane plane, i.e. perpendicular to the membrane normal.

Separating the effects of dye-wobbling from the global rotation of the holding matrix may also be attempted by measuring steady state fluorescence anisotropy during a gradual quenching of fluorescence emission by a quencher (e.g. KI) or by FRET (“quenching-resolved anisotropy, QREA” [17]).

Alternative biological systems for the depolFRET enhancement

As to the biological systems, where the FRET enhancement (or reorientation) can be expected, our present case of dyes tethered through whole mAbs to the cell surface, although it is suitable, may not be the best one. An experimentally measurable parameter for checking the existence of the effect – i.e. the increase in FRET due to the increased matching of donor and acceptor relative orientations – is the anisotropy of sensitized emission, called by us r_{et} , and as a consequence the acceptor anisotropy of the FRET sample, due to its dependence on r_{et} . An impetus for carrying out the present study was our earlier observation that the anisotropy of sensitized emission (r_{et}) for surface tethered dyes, albeit in the majority of cases proven to be very close to zero, in some cases showed significant deviations in the positive

direction. Significantly different than zero transfer anisotropies occurred for mAbs of small (~ 1.0) labeling ratios, for the rather strictly bound Fab fragments and generally for cases where FRET efficiency has been proven to be rather small ($< 15\%$). At well above 30% FRET efficiencies r_{et} stayed generally closely to zero ($< 5\%$). Based on these observations, marked effects can be anticipated for strictly bound dyes having narrow orientation distributions, i.e. static, oriented systems such as dyes tethered to the receptors through Fab fragments, dyes intercalating in the cell membrane (DiI, Bodipy PC, DPH) and engineered visible fluorescein proteins (VFP) [29, 42, 43]. In contrast, the effect is not expected for acceptors of high symmetry (lanthanides, quantum dots, metal nanospheres) [44-46].

FRET as a molecular level switching process

Depolarized excitation enhances FRET by introducing new FRET pathways. In addition to the above treated potential for probing receptor dynamics, excitation with depolarized light can increase the sensitivity of FRET detection because of the involvement of extra FRET pathways, not available under polarized illumination. The effect of depolarized exciting light on FRET formally mimics that of an increased rotational diffusion [12, 13]. Although the enhancement is detectable even in globally isotropic FRET systems such as those on the whole cell surface in a flow cytometer – and probably also in cuvette in a bulk fluorimeter –, special use can be anticipated in microscopy when only a portion of cell membrane can be considered [15, 16, 42]. In this communication we gave an example that sensitivity of FRET detection may be extended already at the level of photoselection of donor population taking part in FRET. In limiting cases of strictly and non-randomly oriented donor-acceptor pairs even selected information transmission via FRET can be imagined at the molecular level, where the donors taking part in FRET are selected based on their polarization state. In this case the FRET pair behaves as a molecular switch (or gate) for information transmission and manipulation [47-49].

DepolFRET with structured light: helicity transfer, 3-dimensional depolarization, rotation by light

The depolarized light beams achieved by the Cornu-depolarizer and the quarter-wave plate are the simplest versions for the kind of light what is called “structured light”: Polarizationally modulated light beams carrying different amount of spin and angular momenta. In appropriate experimental conditions these light types hold the promise for more effective and orientation independent FRET as compared to our present case mainly via 2 mechanisms: (i) Angular momentum (or its projection to the traveling direction of light, called “optical helicity”) conservation [50-53]. (ii) Realization of 3-dimensionally depolarized excitation [54-57].

(i) The presence of angular momentum in the circularly polarized light is evident. As to the Cornu-depolarizer, it acts as a spatial polarization modulator (“pseudo-depolarizer”), by inducing elliptic polarization with periodically changing axis orientation and ellipticity down the laser beam diameter, the time averaged effect of which is detected in the flow cytometer. Consequently, transport of angular momentum can be assumed also in this case. Subsequent to absorption, angular momentum is transferred to the absorber. However, because of thermal relaxation between the absorption and fluorescence emission, one portion of it is given off to the environment of dye. The other portion can be reemitted or can be transferred to the acceptor, but these possibilities require special electronic structure on the part of the absorber: Its emission moment should be capable for two 90° out of phase vibrations in perpendicular directions in a plane i.e. for rotation. Emitters of quadrupole character may fulfill this criterium. With our present dyes this situation is unlikely, but can not be excluded entirely. Rotating dipole emitters hold the promise for a more efficient FRET due to an increased κ^2

independently from the donor-acceptor relative orientation, and also for the transfer of angular momentum (“helicity transfer”) [50-53].

(ii) The depolarization discussed so far, achieved by light beams which are depolarized from whatever reason in a plane is only 2-dimensional. More efficient depolarization of donor emission and of FRET from the donor can be achieved by applying 3-dimensionally depolarized excitation realized e.g. in the focus of a 4π microscope or by the combined action of a longitudinally polarized and a depolarized light beam [54-59].

Another representative of structured light is the one what is called “optical needle”: Axially polarized light when focused by a high numerical aperture objective is converted to a light beam of longitudinal polarization in the focus [58, 59]. Alternately exciting in time with this light needle and with a depolarized light with its plane of polarization perpendicular to the direction of the needle should cover the whole orientational space of the 4π steric angle. The total of the FRET signals acquired with the needle and the depolarized light should correspond to a completely, i.e. to a 3-dimensionally depolarized FRET from the donor.

At the ultimate end of the scale of possible applications of structured light to control FRET stands the possibility for rotating by light the donor molecule (“nano-tweezer”) [60].

Conclusion

Modulation of FRET by donor photoselection has been demonstrated with dyes tethered to the cell surface receptors through mAbs. Correlated FRET enhancements and reductions of anisotropy for sensitized emission have been observed for depolarized excitation modes as compared to excitation with linearly polarized light. The observed effects showed a dependence on the acceptor-to-donor concentration ratio as well as on the type of the donor-acceptor pair. The basic observations of FRET enhancements obtained for hetero-FRET systems are supported by an analogue observation on a homo-FRET system, where increased homo-FRET has been observed upon excitation depolarization.

Depolarized states of the exciting light has been achieved with birefringent crystals operating on the Cornu’s principle, diagonal polarization by a polarizing parallel beam-splitter, and circular polarization by a quarter wave-plate. The simultaneous detection of donor and acceptor anisotropies and the FRET efficiency realized in the „Single laser polFRET” platform made possible the computation of the r_{et} anisotropy of sensitized emission. New parameters having improved sensitivity for probing conformational dynamics, such the „polarized FRET efficiency” T and the anisotropy ratio $r_2/r_{2,\text{av}}$ describing rotations of both the donor and acceptor and FRET, have also been introduced.

Depolarization enhanced FRET can be expected for acceptors having anisotropic orientation distributions with a degree depending on the degree of anisotropy. In addition to improving the sensitivity of FRET detection, conformational dynamics of FRET pairs can be probed without the need for polarized detection by only comparing FRET under depolarized and polarized excitations. The phenomenon of depolarization enhanced FRET can be utilized in flow cytometers and microscopes equipped with conventional „non-polarizing” detection optics after extending them with alternative excitation polarization facilities.

Acknowledgements: Financial support for this work was provided by TÁMOP-4.2.2.A-11/1/KONV-2012-0045 project co-financed by the European Union and the European Social Fund, and OTKA Bridging Fund support OSTRAT/810/213 by the University of Debrecen. One of the authors (L.B.) is wishing to express the appreciation for Imre Péntek (Nagykörös, Hungary) for a fascinating first introduction into the field of wave polarization.

References

1. van der Meer, B.W. 2013. Ch. 3 Förster theory. in FRET - Förster resonance energy transfer: from theory to applications. I. Medinzt, and N. Hildebrandt eds. Wiley-VCH; 1th edition.
2. Jares-Erijman, E.A., and T. M. Jovin. 2003. FRET imaging. *Nat. Biotechnol.* 21(11): 1387-1395.
3. Lakowicz, J.R. 1999. Energy transfer. Ch. 13. In: Principles of Fluorescence Spectroscopy. Kluwer Academic/Plenum Publishers, New York p 368-391.
4. Clegg, R.M. 2009. Förster resonance energy transfer-FRET what is it, why do it, and how it's done. Ch. 1 In: FRET and FLIM techniques. Laboratory techniques in biochemistry and molecular biology. Vol. 33. TWJ Gadella ed., S Pillai , PC van der Vliet series eds. Elsevier p 1-48.
5. Periasamy A., and R.N. Day eds. 2011. Molecular Imaging: FRET Microscopy and Spectroscopy. Academic Press, 1th edition p 1-307.
6. van der Meer, B.W. 1999. Orientational aspects in pair energy transfer. In: Resonance energy transfer. D.L. Andrews, and A.A. Demidov, editors. J. Wiley & Sons, New York. 151-172.
7. van der Meer, B.W. 2002. Kappa-squared: from nuisance to new sense. *Rev. Mol. Biotechnol.* 82: 181-196.
8. van der Meer, B.W. 2013. Optimizing the orientation factor KAPPA-SQUARED for more accurate FRET measurements. Ch. 4 in FRET - Förster resonance energy transfer: from theory to applications. I. Medinzt, and N. Hildebrandt eds. Wiley-VCH; 1th edition.
9. Albrecht, A.C. Polarizations and assignments of transitions: the method of photoselection. *J. Mol. Spectroscopy.* 1961. 6: 84-108.
10. Kliger, D.S., J.W. Lewis, and C.E. Randall. 1990. Orientation and photoselection effects. Ch. 7. In: Polarized light in optics and spectroscopy. Academic Press Inc. Boston, pp. 201-235.
11. Michl, J., and E.W. Thulstrup. 1986. Quantitative aspects of uniaxial alignment. Ch. 4. In: Spectroscopy with polarized light. VCH Publishers, Inc. New York , pp. 171-220.
12. Haas, E., E. Katchalski-Katzir, and I.Z. Steinberg. 1978. Effect of orientation of donor and acceptor on the probability of energy transfer involving electronic transitions of mixed polarization. *Biochemistry.* 17(23): 5064-5070.
13. Steinberg, I.Z., E. Haas, E. Katchalski-Katzir, 1983. Long-range nonradiative transfer of electronic excitation energy. In: Time-resolved fluorescence spectroscopy in biochemistry and biology. R.B. Cundall and R.E. Dale eds., NATO advanced science institutes series A: Life sciences, Springer Science+Business Media, New York, pp: 411-450.
14. Matkó, J., A. Jenei, L. Mátyus, M. Ameloot, and S. Damjanovich. 1993. Mapping of cell surface protein-patterns by combined fluorescence anisotropy and energy transfer measurements. *J Photochem Photobiol B.* 19(1): 69-73.
15. Corry, B., D. Jayatilaka, B. Martinac, and P. Rigby. 2006. Determination of the orientational distribution and orientation factor for transfer between membrane-bound fluorophores using of a confocal microscope. *Biophys. J.* 91: 1032-1045.
16. Sund, S.E., J.A. Swanson, and D. Axelrod. 1999. Cell membrane orientation visualized by polarized total internal reflection fluorescence. *Biophys. J.* 77: 2266-2283.
17. Bene, L., T. Ungvári, R. Fedor, and L. Damjanovich. 2014. Single-laser polarization FRET (polFRET) on the cell surface. *BBA Mol. Cell Res.* 1843: 3047-3064.

18. Dale, R.E., J. Eisinger, and W.E. Blumberg. 1979. The orientational freedom of molecular probes. The orientation factor in intramolecular energy transfer. *Biophys. J.* 26:161-194.
19. van der Meer, B.W., M.A. Raymer, S.L. Wagoner, R.L. Hackney, J.M. Beechem, and E. Gratton. 1993. Designing matrix models for fluorescence energy transfer between moving donors and acceptors. *Biophys. J.* 64:1243-1263.
20. Kliger, D.S., J.W. Lewis, and C.E. Randall. 1990. Devices for control of polarized light. Ch. 3. *In: Polarized light in optics and spectroscopy.* Academic Press Inc. Boston, pp. 27-58.
21. Hodgson, N. and H. Weber. 1997. Polarization. Ch. 3. *In: Optical Resonators. Fundamentals, advanced concepts and applications.* Springer Verlag. London, pp. 115-132.
22. Dörband, B., H. Müller, and H. Gross. 2012. Polarimetry Ch. 51. *In: Metrology of optical components, Vol. 5 In: the series Handbook of optical systems.* ed. H. Gross. Wiley-VCH Verlag-GmbH&Co. pp. 559-616.
23. Françon, M. and S. Mallick. 1971. Birefringent beam-splitters. Ch. 2. *In: Polarization interferometers.* Wiley-Interscience, John-Wiley&Sons Ltd. London, pp. 19-33.
24. Valeur, B. 2002. Fluorescence polarization. Emission anisotropy. Ch. 5. *In: Molecular fluorescence. Principles and applications.* Wiley-VCH, Weinheim. pp. 125-154.
25. Dale, R.E. 1988. Some aspects of excited-state probe emission spectroscopy for structure and dynamics of model and biological membranes. *In: Polarized spectroscopy of ordered systems.* B. Samori' and E.W. Thulstrup eds., Kluwer Academic Publishers, pp. 491-567.
26. Szöllösi, J., S. Damjanovich, M. Balázs, P. Nagy, L. Trón, M.J. Fulwyler, and F.M. Brodsky. 1989. Physical association between MHC class I and class II molecules detected on the cell surface by flow cytometric energy transfer. *J. Immunol.* 143:208-213.
27. Szöllösi, J., V. Hořejší, L. Bene, P. Angelisová, and S. Damjanovich. 1996. Supramolecular complexes of MHC class I, MHC class II, CD20, and Tetraspan molecules (CD53, CD81, and CD82) at the surface of a B cell line JY. *J. Immunol.* 157:2939-2946.
28. Jenei, A., S. Varga, L. Bene, L. Mátyus, A. Bodnár, Z. Bacsó, C. Pieri, R.Jr. Gáspár, T. Farkas, and S. Damjanovich. 1997. HLA class I and II antigens are partially co clustered in the plasma membrane of human lymphoblastoid cells. *Proc. Natl. Acad. Sci. USA.* 94:7269-7274.
29. Gáspár Jr. R., P. Bagossi., L. Bene, J. Matkó, J. Szöllösi, J. Tözsér, L. Fésüs, T.A. Waldmann, and S. Damjanovich. 2001. Clustering of class I HLA oligomers with CD8 and TCR: three-dimensional models based on fluorescence resonance energy transfer and crystallographic data. *J. Immunol.* 166:5078-5086.
30. Bene, L., J. Szöllösi, G. Szentesi, L. Damjanovich, R.Jr. Gáspár, T.A. Waldmann, S. Damjanovich. 2005. Detection of receptor trimers on the cell surface by flow cytometric fluorescence energy homotransfer measurements. *BBA Mol. Cell Res.* 1744:176-198.
31. Lakowicz, J.R. 1999. Fluorescence anisotropy. Ch. 10. *In: Principles of Fluorescence Spectroscopy.* Kluwer Academic/Plenum Publishers, New York, pp. 291-318.
32. Clarke, D., J.F. Grainger. 1971. Measurement of the state of polarization. Ch. 4. *In: Polarized light and optical measurement.* Pergamon Press, Oxford, pp. 118-154.
33. Asbury, C.L., J.L. Uy, and G. van den Engh. 2000. Polarization of scatter and fluorescence signals in flow cytometry. *Cytometry* 40:88-101.

34. Jovin, T.M. 1979. Fluorescence polarization and energy transfer: Theory and application. In: Flow Cytometry and Sorting. M. Melamed, P. Mullaney, and M. Mendelsohn, editors. J. Wiley & Sons, New York. 137-165.
35. Szentesi, G., G. Horváth, I. Bori, G. Vámosi, J. Szöllösi, R. Gáspár, S. Damjanovich, A. Jenei, and L. Mátyus. 2004. Computer program for determining fluorescence energy transfer efficiency from flow cytometric data on a cell-by-cell basis. *Comput. Meth. Prog. Bio.* 75:201-211.
36. Loura, L.M.S. 2012. Simple estimation of Förster resonance energy transfer (FRET) orientation factor distribution in membranes. *Int. J. Mol. Sci.* 13: 15252-15270.
37. Trón, L., J. Szöllösi, S. Damjanovich, S. H. Helliwell, D. J. Arndt-Jovin, and T. M. Jovin. 1984. Flow cytometric measurements of fluorescence resonance energy transfer on cell surfaces. Quantitative evaluation of the transfer efficiency on a cell-by-cell basis. *Biophys. J.* 45:939-946.
38. Szöllösi J., L. Mátyus, L. Trón, M. Balázs, I. Ember, M.J. Fulwyler, S. Damjanovich. 1987. Flow cytometric measurements of fluorescence energy transfer using single laser excitation. *Cytometry* 8:120-128.
39. Kapanidis, A.N., T.A. Laurence, N.K. Lee, E. Margeat, X. Kong, and S. Weiss. 2005. Alternating-laser excitation of single molecules. *Acc. Chem. Res.* 38/7: 523-533.
40. Lesoine, J.F., J.Y. Lee, J.R. Krogmeier, H. Kang, M.L. Clarke, R. Chang, D.L. Sackett, R. Nossal, and J. Hwang. 2012. Quantitative scheme for full-field polarization rotating microscopy using a liquid crystal variable retarder. *Rev. Sci. Instruments* 83/053705: 1-9.
41. Hafi, N., M. Grunwald, L.S. van den Heuvel, T. Aspelmeier, J.-H. Chen, M. Zagrebelsky, O.M. Schütte, C. Steinem, M. Korte, A. Munk, and P.J. Walla. 2014. Fluorescence nanoscopy by polarization modulation and polarization angle narrowing. *Nath. Meth.* 11/5: 579-584.
42. Axelrod, D. 1979. Carbocyanine dye orientation in red cell membrane studied by microscopic fluorescence polarization. *Biophys. J.* 26: 557-574.
43. Rocheleau, J.V., M. Edidin, D.W. Piston. 2003. Intrasequence GFP in class I MHC molecules, a rigid probe for fluorescence anisotropy measurements of the membrane environment. *Biophys. J.* 84:4078-4086.
44. Gaponenko, S.V. 1989. Absorption and emission of light by semiconductor nanocrystals. Ch. 5 In: Optical properties of semiconductor nanocrystals. Cambridge studies in modern optics. P. L. Knight and A. Miller, editors. Cambridge University Press, Cambridge. 84-151.
45. Geddes, C.D., K. Aslan, I. Gryczynski, J. Malicka, and J.R. Lakowicz. 2005. Radiative decay engineering (RDE). Ch. 14 In: Radiative decay engineering. Vol. 8 In: the series Topics in fluorescence spectroscopy. eds. C.D. Geddes, and J.R. Lakowicz, Springer Science+Business Media, Inc. pp. 405-446.
46. Bene, L., G. Szentesi, L. Mátyus, R. Jr. Gáspár, S. Damjanovich. 2005. Nanoparticle energy transfer on the cell surface. *J. Mol. Recognit.* 18: 1-18.
47. Raymo, F.M. 2002. Digital processing and communication with molecular switches. *Adv. Matter.* 14/6: 401-414.
48. Raymo, F.M., and S. Giordani. 2002. All optical processing with molecular switches. *PNAS* 99/8: 4941-4944.
49. Xu, Q.-H., S. Wang, D. Korystov, A. Mikhailovsky, G.C. Bazan, D. Moses, A.J. Heeger. 2005. The fluorescence resonance energy transfer (FRET) gate: A time-resolved study. *PNAS* 18/102(3): 530-535.

50. Babiker, M., C.R. Bennett, D.L. Andrews, L.C. Dávila Romero. 2002. Optical angular momentum exchange in the interaction of twisted light with molecules. *Phys. Rev. Lett.* 89/14: 143601(1-4).
51. Andrews, D.L. 2010. On the conveyance of angular momentum in electronic energy transfer. *Phys. Chem. Chem. Phys.* 12: 7409-7417.
52. Barnett, S.M., R.P. Cameron, A.M. Yao. 2012. Duplex symmetry and its relation to the conservation of optical helicity. *Physical Review A* 86: 013845(1-4).
53. Nieto-Vesperinas, M. 2015. Optical theorem for the conservation of electromagnetic helicity: Significance for molecular energy transfer and enantiomeric discrimination by circular dichroism. *Physical Review A* 92: 023813(1-8).
54. Chen, W., Q. Zhan. 2011. Three dimensional polarization control in 4Pi microscopy. *Optics Commun.* 284: 52-56.
55. Azzam, R.M.A. 2011. Three-dimensional polarization states of monochromatic light fields. *J. Opt. Soc. Am. A* 28/11: 2279-2283.
56. Abouraddy, A.F., K.C. Jr. Toussaint. 2006. Three-dimensional polarization control in microscopy. *Phys. Rev. Lett.* 96: 153901(1-4).
57. Hedde, P.N., S. Ranjit, E. Gratton. 2015. 3D fluorescence anisotropy imaging using selective plane illumination microscopy. *Optics Exp.* #246208: 22308-22317.
58. Roy, T., E.T.F. Rogers, G. Yuan, N.I. Zheludev. 2014. Point spread function of the optical needle superoscillatory lens. *Appl. Phys. Lett.* 104: 231109(1-5).
59. Rogers, E.T.F., S. Savo, J. Lindberg, T. Roy, M.R. Dennis, N.I. Zheludev. 2013. Super-oscillatory optical needle. *Appl. Phys. Lett.* 102: 031108(1-4).
60. Arita, Y., M. Mazilu, K. Dholakia. 2013. Laser-induced rotation and cooling of a trapped microgyroscope in vacuum. *Nat. Comm.* 4/2374: 1-7.

Legend to Figures

Fig. 1 Cartoon illustrating FRET enhancement by excitation depolarization. Due to the orientational restriction of FRET formulated in the „orientation factor”, excitation with depolarized light can be more favorable for FRET than excitation with polarized one, by the fact that in depolarized light more donor orientations are sampled. The magnitude of the expected FRET enhancement is governed by factors such as the degree of orientation randomness, rotational dynamics, and the relative abundance of the donor and acceptor. Orientation distribution of dyes targeted through ligands to membrane receptors – such as the Alexa-labeled receptors in our case – can be substantially anisotropic and their rotational motion highly restricted favoring the occurrence of the FRET enhancement effect. Besides receptor-tethered dyes and VFPs, lipid-intercalating dyes such as DiI, Bodipy PC, and DPH having strongly anisotropic orientation distributions can also be the candidates to show this effect.

Illustrated is that, for anisotropic acceptor orientation distributions (relative to the cell membrane) in polarized light spatial inhomogeneities of FRET can occur on the cell membrane, which can be eliminated by depolarization of the exciting light (blue arrows on the left). Orientation distributions of the donors and acceptors relative to the cell membrane are represented by the double arrows positioned to the north pole and to the equator of the cells represented by grey filled circles (numbered #1-#6). Green filled and empty double arrows represent excited and non-excited donors, red and black filled ones excited and non-excited acceptors. The orientation distributions and the orientation dependence of FRET are represented by strongly simplified manners. All dipoles can assume only two orientations: either parallel or perpendicular to the local membrane plane. On all cells, the donors are randomly distributed, represented by crossed double arrows. Acceptors are oriented either

perpendicular to the membrane plane (cells #1, #4), parallel (cells #2, #5), or randomly (cells #3, #6). FRET is conceived as a two-state switch: it can occur only between parallel donor and acceptor dipoles („closed switch”), and can not between perpendicular ones („open switch”). *Row A:* Excitation by vertically polarized light. From the isotropically oriented donors only the vertical ones are photoselected. Due to the orientation restriction of FRET, while for the perpendicular and parallel orientations of the acceptor only acceptors located on the north pole (cell #1) or the equator (cell #2) of the cells can take part in FRET, for isotropic acceptor orientations (cell #3) in both membrane locations there is some FRET. *Row B:* In depolarized light no spatial FRET inhomogeneity exists (cells #4-#6), regardless of the orientation distribution of the acceptor.

Fig. 2 Optical layout of single-laser polFRET and detected signals. The beam of an Ar⁺-laser in “all-lines” mode is fed into the cytometer through a “Fresnel double-rhomb” polarization rotator (PR) onto which a depolarizer – Cornu, quarter-wave plate, parallel beam-splitter – is mounted. The fluorescence is collected by a lens (L₂), directed after the long-path filter (LPF) by a dichroic mirror beam-splitter (DM) towards the polarization beam-splitter cubes (PBS₁, PBS₂), which together with the respective band-pass filters (BPF₁, BPF₂) constitute the “green (#1)” and “red (#2)” polarized intensity channels.

Fig. 3: Modes of photoselection. In all panels the traveling direction of the exciting light is in the direction of the y axis, the observation is along the x axis. *Panel A:* Horizontally polarized light is used for determining the G-factors, which is used for calculation of anisotropies in the other excitation modes. The photoselected dipoles constitute a cone (green) with the observation direction (x), as the axis of symmetry. In reality there exists another cone in the direction of the (–x) axis, but this is omitted for simplicity. *Panel B:* Vertically polarized light is used for calculating the emission anisotropy and total intensity of the fluorophores. These quantities can be taken as molecular attributes which are independent from the mode of photoselection, and they should be given back also by the other excitation modes. *Panel C:* Diagonally polarized excitation, as a combination of the previous horizontal and vertical ones, rotated by an arbitrary angle θ from the vertical (z) direction. The photoselected dipole ensemble is the superposition of those for the horizontal and vertical polarizations. It can be shown, that the way of calculation of the anisotropy is the same as for the depolarized excitation, independently from θ (see at the end of *Supporting information*). *Panel D:* Depolarized excitation. Formally it can be obtained from the previous polarized and diagonally polarized cases by random rotations of the photon field vectors (blue double arrows) from their original directions in the x-z plane. Consequently the photoselected ensemble can be obtained by rotating the corresponding cones around the y axis. The photoselected ensemble constitute a volume also obtainable from the sphere representing all spatial orientations – the total 4π steric angle – by omitting two conical volumes around the (+y) and (–y) axes [24, 25]. An alternative construction of the photoselected ensemble is by making the horizontal and vertical projections for each field vector and taking into account the corresponding cones with the squares of the projections as intensity weights (see in *Supporting information*). Rotation of polarization direction has been achieved with a Fresnel double-rhomb, depolarization with Cornu#1 and Cornu #2 depolarizers or with a circular polarizer, diagonal polarization by a polarizing parallel beam-splitter.

Fig. 4 FRET enhancement and FRET-mediated loss of acceptor anisotropy under depolarized excitation. Shown are representative flow cytometric polFRET histograms for the A488-L243+A546-W6/32 mAb pair labeling the MHCII+MHCI h.c. receptor pair for excitation with vertically polarized and depolarized light, drawn with thin black and thick red lines,

respectively. Depolarized excitation has been achieved by the Cornu#1-depolarizer in these experiments. *Panel A:* Conventional FRET efficiency E (Eq. 8) is shifted to the right by excitation depolarization. *Panel B:* Anisotropy histograms measured for samples labeled only with acceptor (r_a) are practically located on the same mean with the two excitations. If anisotropy for the depolarized case would be computed the same way as for the polarized one, c.a. half the values should be obtained. r_a is a reference when FRET is assessed from acceptor anisotropy. *Panel C:* The relative decrease of acceptor anisotropy (Eq. 12) measured in the presence of FRET r_a' as compared to its value without FRET, r_a is larger for depolarized excitation than for the polarized one, reenforcing the observation that depolarization enhances FRET efficiency E . *Panel D:* Another quantity, the directly measured anisotropy r_2 of the acceptor channel (Eq. 14) can also be used for probing FRET. This is a more sensitive indicator than r_a' because it contains a contribution also from the donor anisotropy, in contrast to r_a' from which the contribution of donor is separated. Although, r_2 is properly referenced to the average anisotropy of the donor and acceptor both measured in the acceptor channel (Eq. 13, not indicated), as an approximation it can also be referenced to the pure acceptor anisotropy r_a , because the donor contribution is generally small. *Panel E:* Reduction in anisotropy of sensitized emission under depolarized excitation. Anisotropy of sensitized emission of acceptor, r_{et} (Eq. 11) which is not zero for polarized excitation – albeit it is much smaller than that of direct emission, r_a – has been reduced to zero under depolarized excitation. That for polarized excitation the anisotropy of sensitized emission is not zero is a direct proof for that the relative orientation of the donor and acceptor is not random for this donor-acceptor pair. In contrast, under depolarized excitation the zero r_{et} means that the relative orientation is randomized leading to new FRET pathways, and consequently, enhanced FRET efficiency. *Panel F:* Increased „polarized FRET efficiency” T under depolarized excitation. Another way for the joint description of FRET efficiency and the anisotropy of sensitized emission is via the „polarized FRET efficiency” T . This quantity can be obtained by expressing the FRET efficiency E from Eqs. 13, 14 as functions of the measurable anisotropy ratios either r_a'/r_a or $r_2/r_{2,av}$ and with the anisotropy of sensitized emission as an assumed input constant. The two measures of FRET, E and T , coincide whenever r_{et} is zero. Otherwise, possible deviations of r_{et} from zero are transformed into corresponding deviations of T and E : T under-estimates E for positive r_{et} and upper-estimates it for negative r_{et} . While for polarized excitation T is smaller than E , indicating that r_{et} is not zero, for depolarized excitation T is close to E , indicating a vanishing r_{et} .

Fig. 5 Excitation depolarization sensitizes FRET dependence of the combined anisotropy r_{2av} , and the „polFRET efficiency” T . Shown are representative flow cytometric polFRET dot-plots for the data of Fig. 3 – i.e. for the A488-L243+A546-W6/32 mAb pair – for excitation with vertically polarized and depolarized light, drawn with black and red dots, respectively. *Panels A, B:* For vertically polarized excitation both the anisotropy r_2 (Panel A) and „polFRET efficiency” T (Panel B) depend only weakly on the conventional FRET efficiency E . *Panels C, D:* For depolarized excitation both the anisotropy r_2 (Panel C) and „polFRET efficiency” T (Panel D) depend rather strongly on the conventional FRET efficiency E . The stronger dependence can be attributed to the observation that sensitized emission is totally depolarized under depolarized excitation as compared to the polarized one.

Fig. 6 Increased homo-FRET under depolarized excitation. Homo-FRET has been quantified by the relative decrease of anisotropy of the sample labeled with both the A546-L368 and A456-W6/32 mAbs as compared to the intensity-weighted average of the anisotropies for the corresponding singly-labeled samples (Eqs. 12s, 13s *Supporting information*). Because both mAbs bind to the same MHC I molecule, large proximity of mAbs, and as a result, high homo-

FRET can be expected in this case. Vertical polarization is illustrated with thin black line, depolarized one – realized with the Cornu#1 depolarizer – with thick red line. *Panel A:* Flow cytometric histogram of homo-FRET enhancement (η) obtained in the depolarized light is shifted to the right as compared to the one in vertically polarized light, reporting on a substantial homo-FRET increase. The increase in homo-FRET, similarly to the case of hetero-FRET, is expected due to the more favorable mutual orientations of the donor – the primarily photo-excited dyes – and acceptor dipoles in depolarized illumination. *Panel B:* Anisotropy histograms for the A456-L368-labeled sample, necessary for the computation of the reference average anisotropy. The mean values obtained with the two polarization modes are almost the same, as expected, however the widths of the curves are substantially different. The slight differences in the mean anisotropies can be attributed partly to possible optical path differences between the polarization modes described by different G-factors and/or aperture depolarization factors – the $a(\psi)$ -factor in the formulae for total intensity, Eqs. 2, 4 –, partly to a homo-FRET increase even on the singly-labeled samples. The larger histogram widths belonging to the depolarized case can be attributed to the intensity loss in the depolarizer. *Panel C:* Anisotropy histograms for the A456-W6/32-labeled sample, the other component for the average anisotropy. *Panel D:* Anisotropy histograms for the homo-FRET sample, double-labeled with the A456-L368 and A456-W6/32 mAbs, from which with referencing to the corresponding averages the homo-FRET enhancement curves on Panel A have been deduced. Although both histograms are shifted to the left of the corresponding averages indicating that homo-FRET is present in both excitation modes, the larger shift belongs to the depolarized mode indicating that homo-FRET is larger in this mode.

Fig. 7 Depolarized excitation speeds up intensity decay of anisotropies. The increased homo-FRET under depolarized excitation manifests itself also at the level of single cells, namely in the increased decay rates – „sensitization” – of the anisotropy vs. total intensity (i.e. dye concentration) curves. Shown are flow cytometric „anisotropy vs. total intensity” scatter plots (dot-plots) for the data of Fig. 5. Here anisotropy and intensity variations are supplied in a „natural way”, by the biological variance of the cells. In all panels anisotropies decrease with intensity at higher rates under depolarized illumination. Vertically polarized and depolarized excitations are illustrated with black and red dots, respectively. *Panels A-D:* „Anisotropy vs. total intensity” dot-plots for the A456-L368- and A456-W6/32-labeled samples. *Panels E, F:* „Anisotropy vs. total intensity” dot-plots for the A456-L368+A456-W6/32 double-labeled homo-FRET sample.

Table 1. Comparison of effects of excitation with polarized and depolarized light exerted on the polFRET parameters on the surface of JY B-lymphoblast cells: Cornu#1 depolarizer

Donor (A488-conjugated)		Acceptor (A546-conjugated)		Samples labeled with only donors or acceptors								Double-labeled (FRET) samples						
mAb	Antigen	mAb [*]	antigen	L _d [*]	L _a [*]	α [†]	c _a /c _d [‡]	r _d	r _a	r _{2,av} [#]	r _{a,av} [#]	η [#]	E [§]	T [§]	r ₂	r _a [']	r _{et}	δr ₂ ^{&}
													(%)					
Part A, vertical polarization																		
L368	β ₂ m			2.03			3.48 ±0.90	23.7 ±1.1		18.2 ±0.6	-	-	41.1 ±3.5	23.7 ±2.1	16.6 ±0.4	15.9 ±0.4	11.6 ±1.4	8.4 ±0.7
W6/32	MHCI h.c.	L243 [*]	MHCII, DRα	2.1	4.4	0.79 ±0.11	0.503 ±0.09	18.8 ±0.3	17.6 ±0.4	18.1 ±0.4	-	-	23.7 ±1.2	13.4 ±1.2	14.8 ±0.1	13.6 ±0.5	8.4 ±1.0	18.5 ±1.7
L368 +W6/32	β ₂ m+ MHCI h.c.			2.07			0.46 ±0.12	18.7 ±0.2		18.1 ±0.3	-	-	25.0 ±2.2	12.5 ±2.8	14.8 ±0.2	14.4 ±1.2	8.0 ±1.8	18.2 ±2.0
Part B, vertical polarization																		
		L368	β ₂ m		3.7		0.07 ±0.04		37.3 ±3.4	27.0 ±2.4	-	-	8.4 ±1.0	5.6 ±1.4	20.7 ±0.8	26.2 ±3.3	9.7 ±1.7	22.5 ±4.0
L243	MHCII, DRα	W6/32	MHCI h.c.	1.2	1.8	0.79 ±0.11	0.41 ±0.19	18.8 ±0.3	26.4 ±1.9	24.1 ±1.6	-	-	23.8 ±1.5	11.0 ±2.5	19.3 ±0.1	19.2 ±0.7	7.7 ±1.4	19.3 ±4.6
		L368 +W6/32	β ₂ m+ MHCI h.c.		2.75		0.56 ±0.11		23.6 ±0.2	22.6 ±0.5	28.2 ±2.5	17.5 ±7.1	21.1 ±1.0	12.3 ±2.6	19.1 ±0.1	19.2 ±0.4	10.4 ±3.5	15.6 ±1.6
Part C, Cornu#1 depolarizer																		
L368	β ₂ m			2.03			3.64 ±0.88	18.5 ±0.3		10.4 ±0.7	-	-	42.7 ±4.1	30.2 ±2.5	10.4 ±0.7	7.8 ±0.7	-1.3 ±2.4	20.5 ±6.2
W6/32	MHCI h.c.	L243	MHCII, DRα	2.1	4.4	0.56 ±0.05	0.53 ±0.09	11.8 ±0.4	12.0 ±0.9	13.4 ±1.3	-	-	26.0 ±1.0	25.2 ±3.3	9.3 ±0.4	7.1 ±0.2	0.6 ±1.6	29.6 ±4.9
L368 +W6/32	β ₂ m+ MHCI h.c.			2.07			0.44 ±0.08	12.3 ±0.3		13.4 ±1.3	-	-	30.6 ±2.0	23.3 ±3.4	9.3 ±0.4	7.1 ±0.2	0.6 ±1.6	29.7 ±5.2
Part D, Cornu#1 depolarizer																		
		L368	β ₂ m		3.7		0.07 ±0.03		32.7 ±2.9	24.1 ±2.4	-	-	10.4 ±0.5	13.7 ±2.5	15.2 ±2.7	16.7 ±1.7	-7.4 ±7.6	32.5 ±1.9
L243	MHCII, DRα	W6/32	MHCI h.c.	1.2	1.8	0.56 ±0.05	0.37 ±0.14	12.0 ±0.4	24.6 ±0.3	20.9 ±0.7	-	-	27.2 ±1.3	24.2 ±4.2	12.7 ±0.7	11.8 ±0.6	-0.5 ±2.9	33.6 ±12.3
		L368 +W6/32	β ₂ m+ MHCI h.c.		2.75		0.54 ±0.07		16.8 ±1.2	16.6 ±1.1	26.7 ±2.4	35.4 ±6.0	25.5 ±2.0	28.6 ±5.0	12.3 ±0.7	11.2 ±0.5	1.5 ±4.8	24.6 ±6.1

^{§)}L designates the dye-per-protein labeling ratio (D/P). The numbers for the cases when 2 donor or acceptor mAbs are used are the averages of the respective labeling ratios.

^{†)}Because α expressing relative sensitivity of the donor and acceptor channel depends on the optical alignment of the flow cytometer, it can be subjected to day-to-day variations even for a given donor-acceptor pair. All values in the table are averages for 3 different measurements (\pm errors in the mean, SEM) subjected to slightly different optical alignments.

^{‡)}Acceptor-to-donor surface dye concentration fractions are determined from total intensities I_{1d} , I_{2a} measured on samples labeled with only donor and acceptor, according to $c_a/c_d \equiv I_{2a}/(\alpha \cdot I_{1d})$. The fractional occupancy of the labeled receptors can be obtained from these numbers by taking into account the respective labeling ratios (L) as $B_a/B_d \equiv (c_a/c_d) \cdot (L_d/L_a)$.

^{#)} $r_{2,av}$ is intensity weighted average of the anisotropies for the donor and acceptor both measured in the acceptor channel. It is important for the calculation of the „polarized FRET efficiency” T (Eqs. 13, 14). $r_{a,av}$ is intensity weighted average of the anisotropies for the acceptor labeled L368 and W6/32 mAbs. It is important for the calculation of the homo-FRET efficiency η , which is calculated as the relative decrease of the anisotropy measured for the sample labeled with both L368 and W6/32 referenced to the average anisotropy of these mAbs, $r_{a,av}$ (Eqs. 12s, 13s *Supporting information*).

^{§)}FRET efficiencies, the ratiometric, total intensity based E and the acceptor anisotropy based T („polarized FRET efficiency”), are computed according to Eqs. 8, 16.

^{&)} δr_2 is defined as the relative decrease of r_2 as compared to $r_{2,av}$ and expressed on the % scale: $\delta r_2 \equiv (1 - r_2/r_{2,av}) \cdot 100\%$.

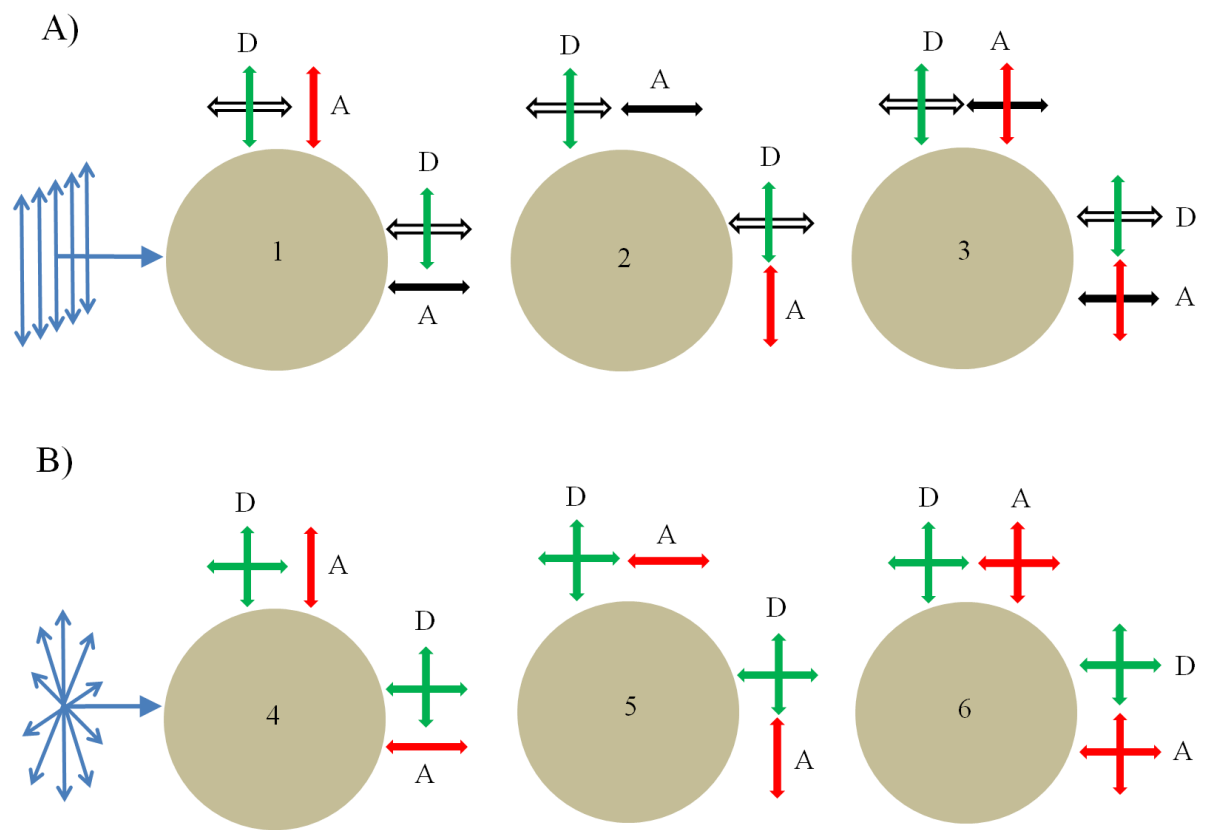


Figure 1

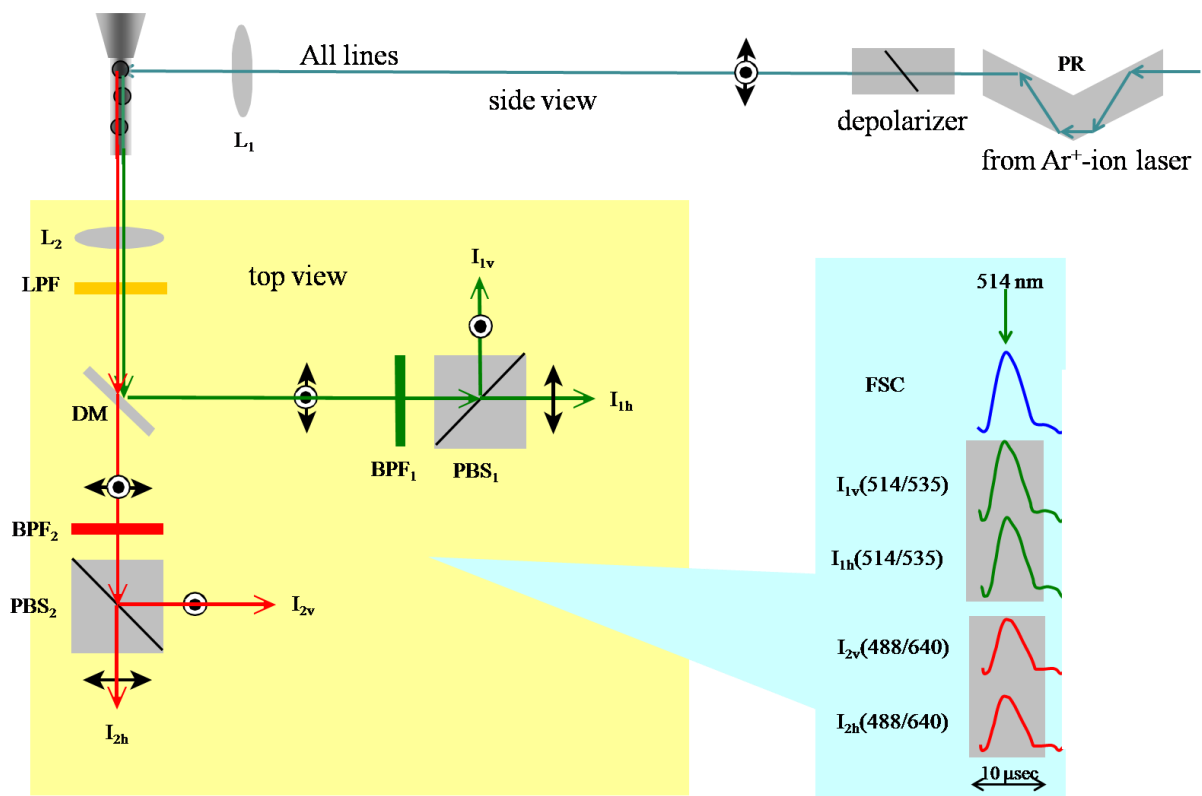


Figure 2

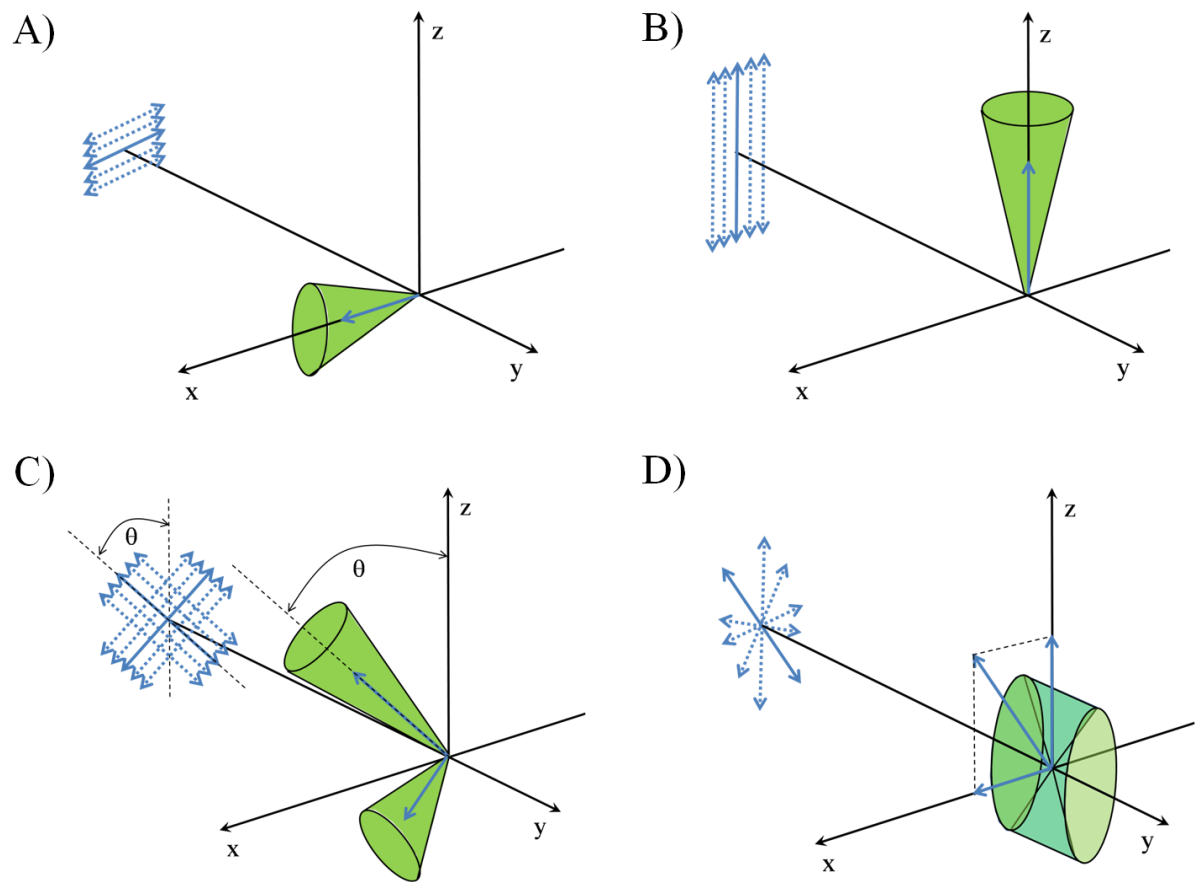


Figure 3

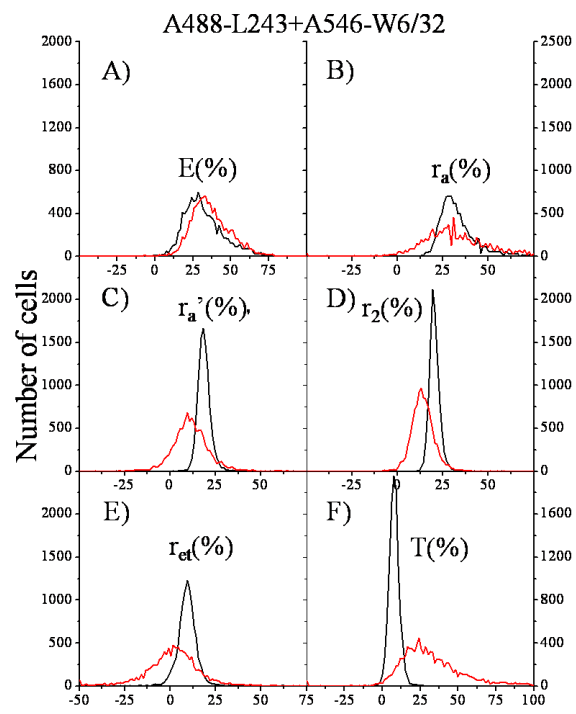


Figure 4

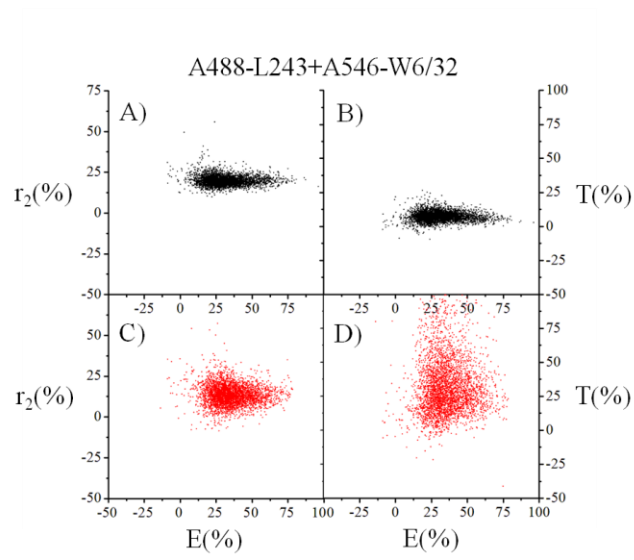


Figure 5

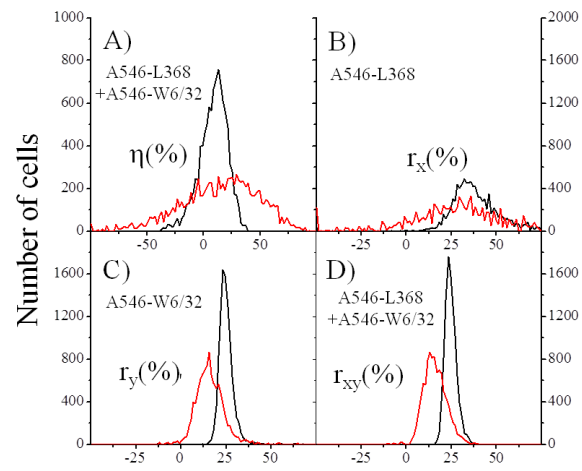


Figure 6

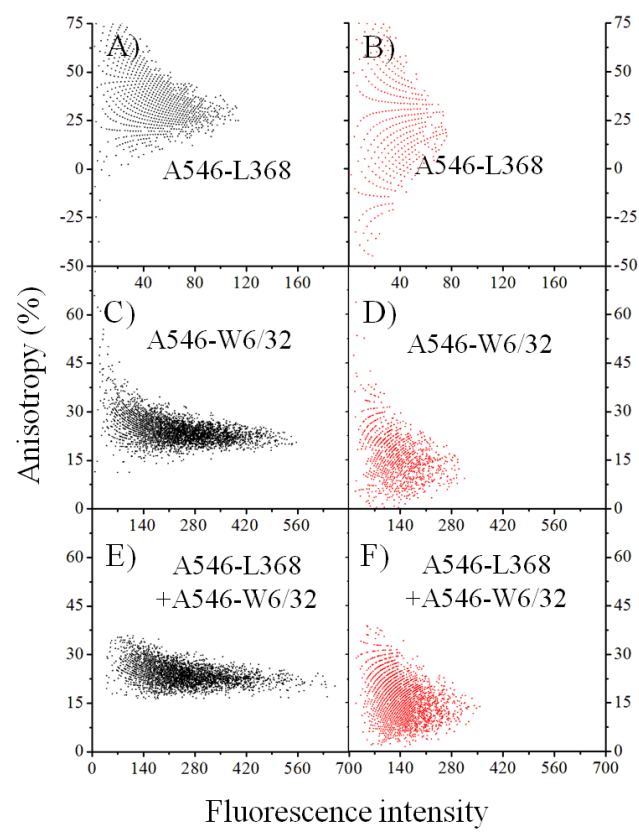


Figure 7